Structural studies of the brass ingots from the Shcherbet historical complex of the Lower Kama region: neutron diffraction and tomography studies

A.Zh. Zhomartova*,[1,2,3], E.F. Shaykhutdinova[4,5,6], B.A. Bakirov[1,5], S.E. Kichanov[1], D.P. Kozlenko[1], A.G. Sitdikov[4,5]

[1]Joint Institute for Nuclear Research, Dubna, Russia

[2]L.N. Gumilyov Eurasian National University, Astana, Kazakhstan

[3]Institute of Nuclear Physics Ministry of Energy of the Republic of Kazakhstan, Almaty, Kazakhstan

[4]Institute of Archaeology named after A.Kh. Khalikov of the Tatarstan Academy of Sciences, Kazan, Russia

[5]Kazan Federal University, Kazan, Russia

[6]Kazan National Research Technical University named after A.N. Tupolev, Kazan, Russia

E-mail: zhomartova@jinr.ru

The structural characteristics and phase composition of several ancient brass ingots obtained in the archeological Shcherbet complex has been studied using neutron diffraction and tomography methods. The XRF analysis and neutron diffraction provide high zinc content up to 30 wt.%. The neutron tomography yielded 3D data of the spatial distribution of chemical elements in the brass alloy of the studied ingots, as well as inner voids and cavities as a possible result of the gas output during casting process. The patina, as a cuprite phase, occupy volumes to 8 % of the volumes of the ingots.

Keywords: neutron diffraction; neutron tomography; brass ingots; the Shcherbet complex

Introduction

Now, the problems of origin, chronology, and ethnocultural community of the so-called Imenkovo historical culture monuments of the VI-VII centuries are of interest for the medieval history of Eastern Europe [1]. This historical cultural region occupied a territory from the Urals to the modern Penza region of Russia. One of the archaeological excavations of this cultural and historical formation is the Shcherbet complex. The ancient settlement is located 3.5 km northwest of the former village of Shcherbet, Spassky District of Tatarstan at an area of ~ 120000 m^2 [1]. The results of archeological works leave no doubt that this monument is a trade and craft settlement of the Imenkovo population of the Lower Kama region.

Brass and bronze ingots used as foundry billets are known since ancient times throughout Europe and North Africa. They became even more widespread in the Late Roman time and reached their maximum in the Viking Age. Possibly prototyped by Late Roman golden bars being collected as taxes, the non-ferrous ingots appeared in the Middle Volga region in the very beginning of the Migration period together with new groups of migrants from the South-West. Those ingots are of similar shape and weight, and were made in special casting molds in a shape of rods (sticks) with a triangular or quadrilateral section and look very similar to those that were in use on the territory of the Roman Empire. Once appeared in the region in the 3rd-4th c., they were in use during three centuries [2].

Among the archaeological materials found in the Shcherbet complex are the remains of a foundry workshop with a hoard of 67 triangular rods as the brass ingots of about 18 cm long and weighing $88-111$ g [3]. According to written records, copper alloys were brought in separate pieces, sold by weight, in the form of various scraps packed in barrels, in the form of wire, boilers, and other products [1, 4]. It is believed that the ingots were raw materials for jeweler production and served as a means of storing metal intended for further use [5]. It is discussed that brass and bronze ingots, along with furs, are representatives of goods supplied from the Kama region to Bulgaria and further to the East and West parts of Europe. The wide distribution of the ingots may indicate their transportation not only by wheeled transport but also by boats on the waterways.

Written source evidence together with archaeological data on medieval mining and metallurgy on the territories of modern Russia and Europe provide us to trace the probable ways of raw materials entering the workshops of the Shcherbet historical complex. The founded ingots allow us to study the connection between metal and an ore source in the Imenkovo cultural area. The shape, dimensions, and chemical composition of ingots indicate that they are produced at the same time and in the same place [1]. The source of copper material close to the Shcherbet complex could be the copper sandstones of the Ural Mining and Metallurgical region, located mainly on the territory of the Kama region, and as well as copper ore deposits of the Central Asian region. More accurately correlate the ingot with the ore source request a comparison of the composition of ingots alloys and ores of the mining zone of brasses and bronzes of that time. Recently, the traditional

X-ray fluorescence analysis, electron microscopy, and metallography methods have been successfully supplemented the neutron non-destructive probes [6]. First of all, this is due to the absence of restrictions on the depth of infiltration into the thickness of the metal sample [7–9]. Additional advantages of neutron methods, including a noticeable difference in contrast between different metals and high penetration ability, show a fundamental difference in the nature of the interaction of neutrons with matter compared to X-rays. The neutron diffraction method provides detailed structural data of the chemical and phase content, the neutron tomography allows us to study the spatial distribution of chemical components inside the large metal objects [10, 11]. In our work, we present neutron tomography and diffraction data for the non-destructive identification of the composition of several copper ingots of the Shcherbet complex.
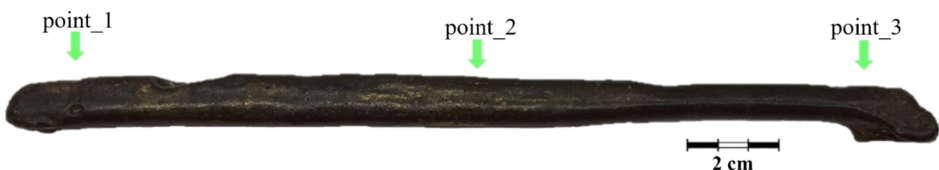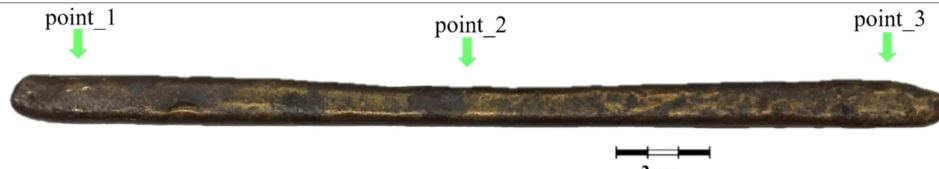
Materials and Methods

Sample description

For our neutron studies three representatives of archaeological brass ingots were selected. The photos of chosen ingots are shown in Table 1. We labeled samples as Sample 1, Sample 2 and Sample 3. All ingots have an elongated rod shape with an average thickness of about 1 cm, the length of the Sample 1 and Sample 2 is about 18 cm, and the Sample 3 is ~ 7 cm.

All the metal samples are covered with a dark coating or patina. The color of the patina may indicate cuprite on the surface of copper items. Also, the scanning points in the neutron diffraction experiments are marked in the photos.

Table 1.
The photos of the studied metal ingots. A scale bar for each sample is shown.

Sample	Photos of brass ingots
1	
2	
3	

Neutron Diffraction

The phase and composition analysis of inner volumes of the ingots were performed by means of neutron diffraction using the DN-12 neutron diffractometer [12, 13] at the IBR-2 powerful pulsed reactor (Frank Laboratory for Neutron Physics, JINR, Dubna, Russia). At a scattering angle of $2\theta = 90°$, powder diffraction data were obtained. For these scattering angles, the resolution of the diffractometer at a wavelength $\lambda = 2$ Å was $\triangle d \setminus d = 0.025$. For additional measurements of various parts of the ingots, a cadmium collimator with a slot diameter of 5 mm was used, which made it possible to study the phase composition of several parts of the ingots (Table 1): point_1, point_2, point_3. Diffraction data processing was performed by the Rietveld method using the Fullprof software program [14]. The characteristic exposition time for one neutron pattern was 30 min.

Neutron Tomography

To obtain data on the internal structure of the ingots, studies were carried out at a specialized experimental station for neutron radiography and tomography [15, 16] at channel 14 of the IBR-2 pulsed reactor. Neutron radiographic images of objects were obtained using a detector system based on a ^{6}LiF/ZnS scintillation screen with image registration by a highly sensitive video camera with HAMAMATSU CCD chip [17]. To study the internal structure of archaeological objects, a number of neutron radiographic experiments were conducted, the result of which was a set of 360 angular projections of the objects under study, with a rotational step of $0.5°$. Due to the high neutron flux, the exposure time for recording one neutron image is only 10 s. Using the ImageJ program, the image data were normalized to the image of the falling neutron beam, after correcting the image with the dark current of the camera [18]. The STP (SYRMEP Tomo Project) software package was used for tomographic reconstructions [19]. A three-dimensional (3D) model obtained by this method is an array of data consisting of three-dimensional voxels (pixels) that characterize the degree or coefficient of attenuation of the neutron beam at a specific point in the sample under study. The size of one voxel of the image was $(52 \times 52 \times 52)\mu m^3$. The attenuation of the neutron beam matches to the scattering and absorption losses within the material [17]. The visual representation and analysis of reconstructed three-dimensional data were executed using the VGStudio MAX 2.2 software developed by Volume Graphics (Heidelberg, Germany).

X-ray Fluoresce Analysis

Elemental analysis on the surface of the ingot was carried out by a non-destructive X-ray fluorescence method on a portable 5i Tracer research-grade spectrometer (Bruker). The excitation source was a 4W X-ray tube with a rhodium mirror. In the operating mode, the voltage of $6-50$ kV and the current range of $4.5-195$ μA were automatically regulated.

Results and discussion

XRF analysis and neutron diffraction

The analysis of the elements and chemical composition of the surface of studied ingots was performed as is. It was found that all studied coins were made from copper-based alloys like CuZn. It is known, zinc was added to the copper for rich yellow-gold color, and copper alloy material became more harder and durably in comparison with bronze. The zinc concentrations based on the XRF analysis data are 14.6 % for ingot Sample 1; 20.7 % in Sample 2; 5.3 % for Sample 3. Small concentrations of tin in the range 0.05 – 0.67 % and lead in the range 0.46 – 0.77 % were observed.

However, the zinc concentration on the surface of ingots may differ from the element context in the entire volume of the object. Due high penetration of neutrons inside a volume of metal samples, the neutron diffraction can provide the requested structural data for studied ingots. We collected typical spectra for copper-based alloys, where dominant phases are cubic copper and patina phases [20]. As an example, a neutron diffraction pattern of Sample 3 brass ingot is shown in Figure 1. Most intense diffraction peaks correspond to the cubic phase of copper with the space group $Fm\bar{3}m$. The lattice parameter of this phase is a = 3.630(3) Å. According to Vegard's law, the lattice parameter of mono-phase alloy changes linearly with the ligand element concentration [21]. The zinc mass contents in the brass ingots were calculated from neutron diffraction data. The comparison diagram of the mass concentration of zinc in the studied ingots and different points is presented in Figure 2. It can be seen that the zinc content in the volumes of ingots is in the range 11.5(5) – 32.1(6) %. The obtained values are higher in compare to X-ray fluorescence analysis results. We can assume that this divergence in the results is due to the loss of zinc on the ingots surface in reason to the evaporation of zinc oxides during prolonged interaction with the soil and airs during historical occurrence. A similar effect has already been described earlier [22, 23].

Several weak diffraction peaks in the neutron diffraction pattern (Figure 1) are indexed as cuprite phases Cu_2O. The crystal structure of this patina phase is described by space group $Pn\bar{3}m$ with lattice parameters a = 4.256(5) Å, b = 4.256(5) Å, c = 4.256(5) Å. The calculated from neutron diffraction data volume fraction of the cuprite phase was fall in the range $\sim 8 - 12$ % by volume.

Neutron tomography

The spatial distribution of the zinc ligand inside the brass ingots can be investigated using neutron tomography method. A rather high difference in the neutron attenuation coefficients of copper and zinc is reason of a good neutron radiographic contrast in neutron radiography experiments. Several virtual slices of the reconstructed tree-dimension (3D) model of the Sample 1 brass ingot shown in Figure 3. Cracks and small voids are clearly evident on the restored model. It is interesting the neutron attenuation coefficient inside the ingot volume is
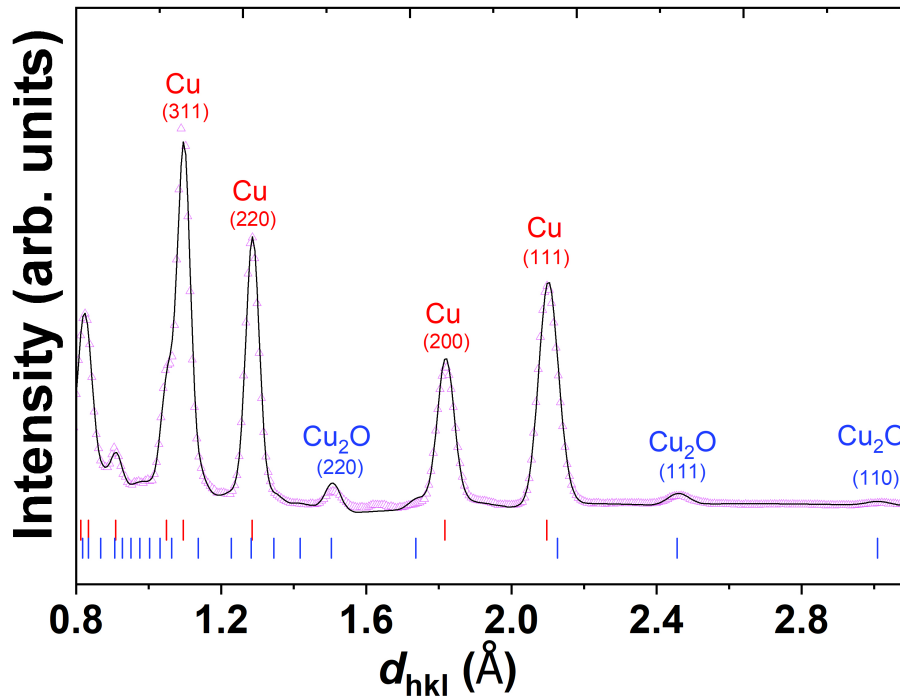
Figure 1. Neutron diffraction patterns of the Sample 3 brass ingot. Experimental points and calculated profile are shown. The marks below represent the calculated positions of the Bragg peaks of the copper and cuprite phases. The corresponded peaks and those indexing are labeled.
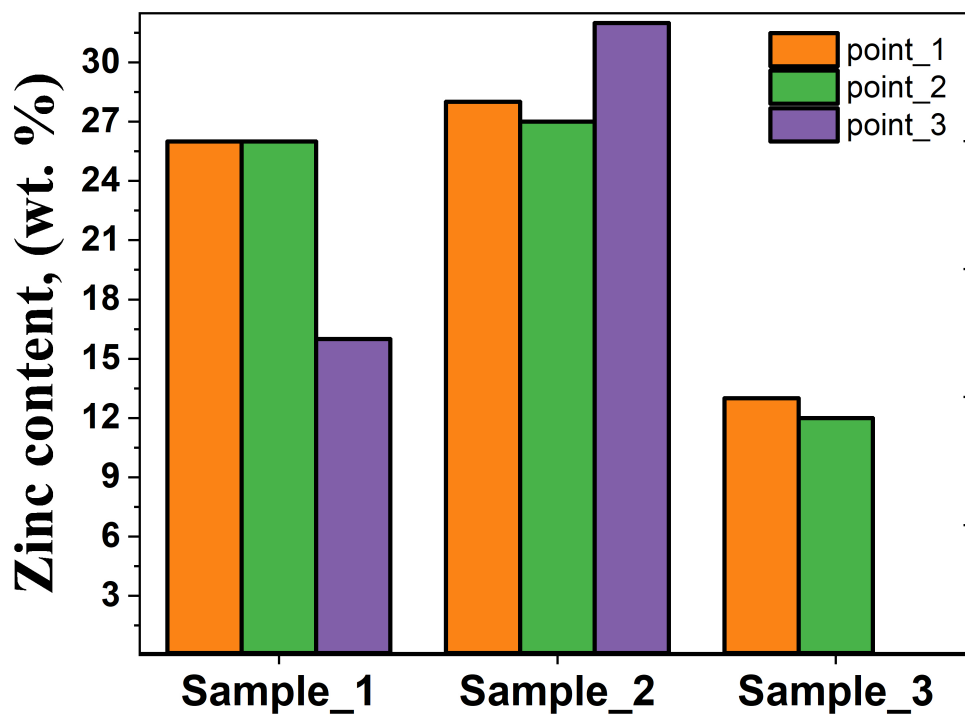

Figure 2. The diagram of the zinc content in the brass ingots based on neutron diffraction data. The average errors in the determination of zinc concentration does not exceed 0.5 wt.%.

heterogeneous. This result and the high zinc content in the studied ingots indicate indirectly a possible ligation of the initial copper ore during melting and some technological features of insufficient mixing of zinc and copper. A patina cuprite phase is clearly observed on the surface on the ingot Sample 1. We can calculate

some bulk parameters from neutron tomography data. The whole volume of the brass ingot Sample 1 consists 11681800 voxels, which equal to 10661.7(1) mm^3. The patina volume is 92980 voxels, or 84.9(1) mm^3.
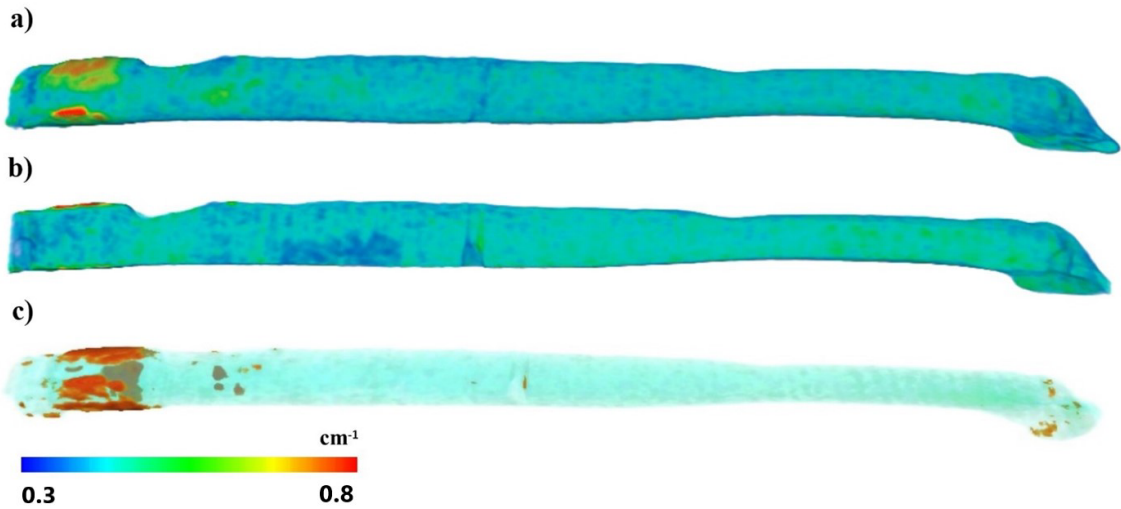

Figure 3. a) The 3D model of brass ingots Sample 1, which was reconstructed from neutron tomography data. b) the longitudinal virtual slice of the reconstructed 3D model of the brass ingot Sample 1. c) The transparent presentation of 3D model of a brass ingot with patina phase labeling. The corresponding scales of the neutron attenuation coefficient from low to high are shown.

The reconstructed 3D model of the ingot Sample 2 is shown in Figure 4. A similar view with Sample 1 is observed for Sample 2. The zinc-poor areas look like some small grains or inclusions inside a volume of copper alloy. It can be assumed about the melting of copper ore and some crumbs or chips of zinc-rich material. It can be seen in Figure 3 that there is slightly less zinc content in the middle part of the ingot than at the edges. This is also confirmed by neutron diffraction data (Figure 2). The volume of Sample 2 ingot consists of 11002991 voxels or 10042.1 mm^3.
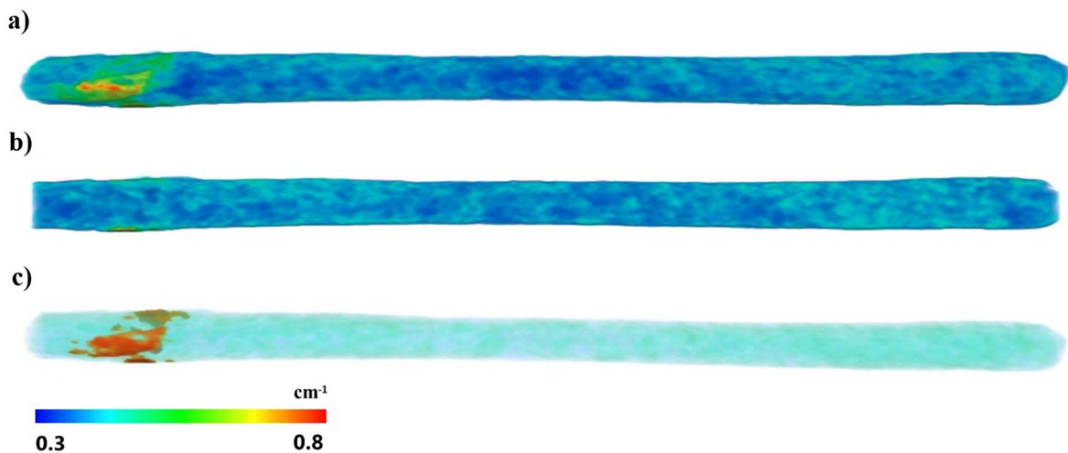

Figure 4. a) The reconstructed 3D model of brass ingots Sample 2. b) The longitudinal virtual slice of the reconstructed 3D model of the brass ingot Sample 2. c) The transparent presentation of 3D model of a brass ingot with patina phase labeling. The corresponding scales of the neutron attenuation coefficient from low to high are shown.

An interesting situation is observed for the Sample 3 (Figure 5). An interesting situation is observed for the last Sample 3. A rather large crack or elongated

cavity was found at one edge of the ingot (Figure 5b). The volume of this cavity in the Sample 3 ingot is 55.7 mm^3. These cavity can be a product of the release of associated gas during the casting process [24]. The distribution of zinc in the copper alloy of the ingot is also heterogeneous, but unlike previous studies, there is a predominant spatial distribution of zinc-rich volumes to one of the edges of the ingot (Figure 5b). Thick near-surface layers of patina are clearly evident on the surface of the ingot Sample 3 (Figure 5c). The thickness of the patina layer reaches up to 1 mm. The calculated volume of the patina component in the ingot Sample 3 is 1502047 voxels or 560.6 mm^3. A comparative diagram of the calculated fraction of patina of the studied ingots is shown in Figure 6.
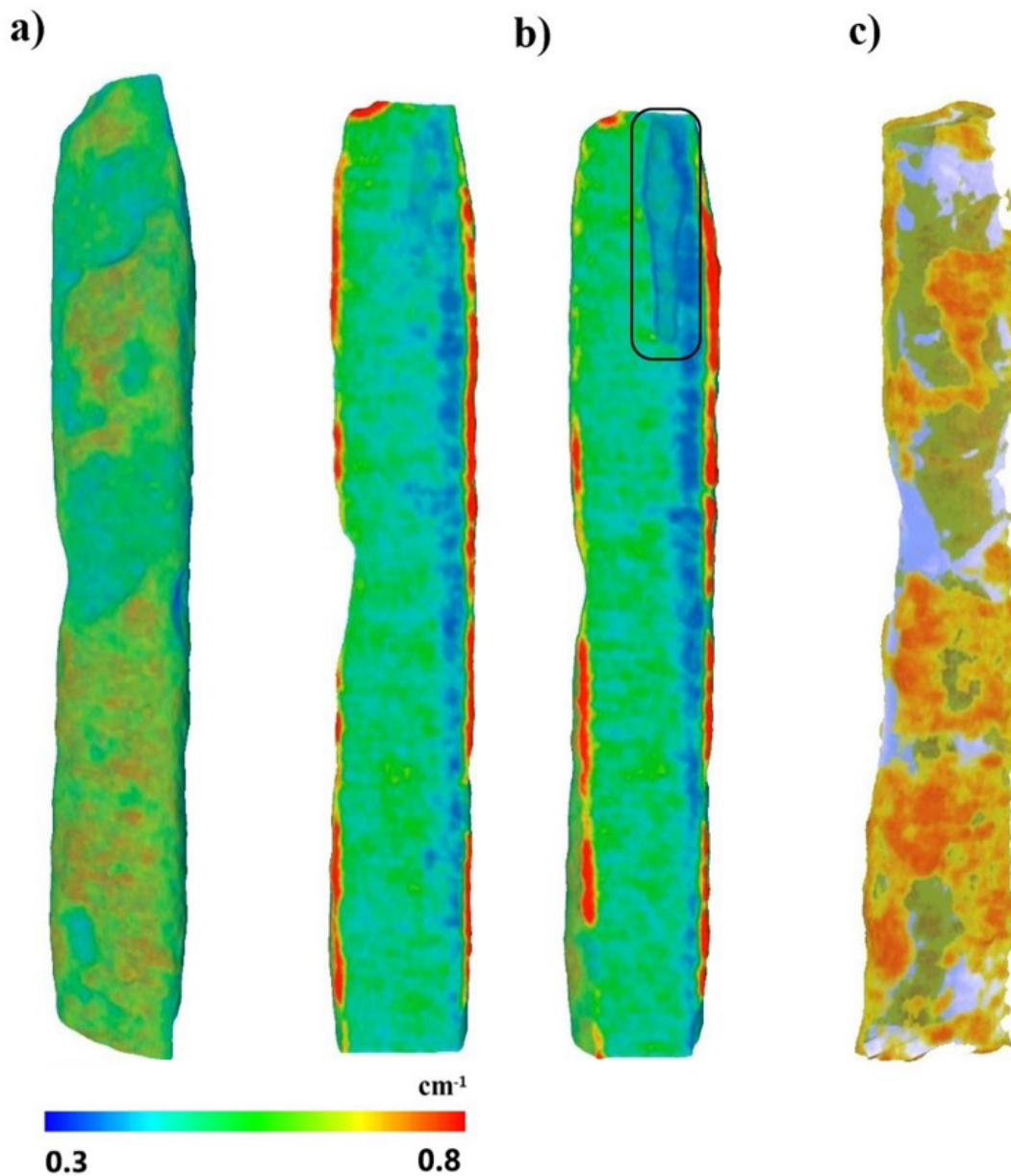

Figure 5. a) The reconstructed 3D model of brass ingots Sample 3. b) The longitudinal virtual slice of the reconstructed 3D model of the brass ingot Sample 3. The inner cavity is labeled. c) The transparent presentation of 3D model of a brass ingot with patina phase labeling. The corresponding scales of the neutron attenuation coefficient from low to high are shown.
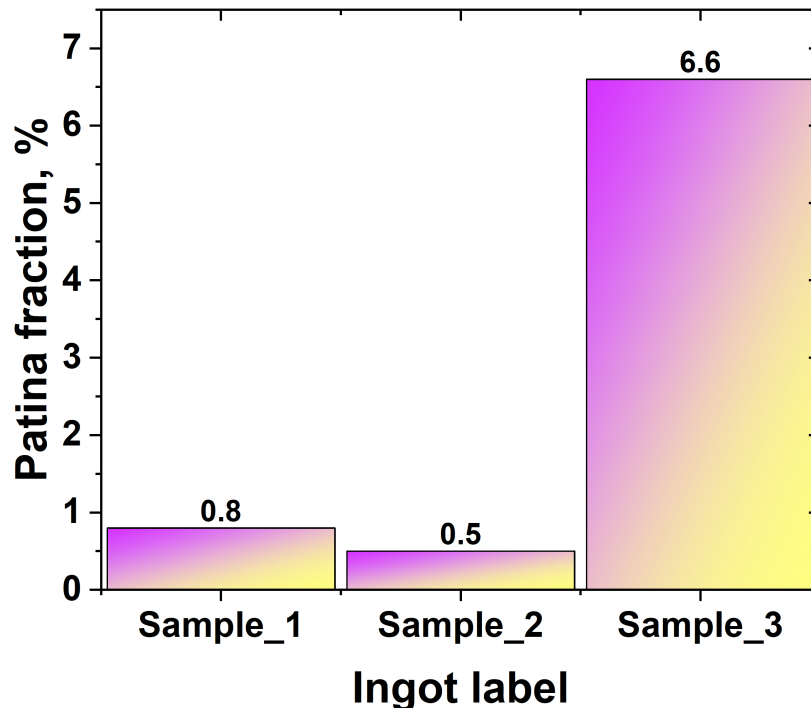
Figure 6. The diagram of the patina volume fraction at the studied ingots based on neutron tomography data.

Conclusions

In our work, we had study the phase composition and spatial distribution of the phase components of three brass ingots from the Shcherbet archeological complex by neutron diffraction and tomography methods. A high zinc content was found in the bulk of the copper alloy of the ingot. A cuprite patina is formed on the surface of the ingots, its spatial distribution is highlighted. The 3D models, the zinc concentration, the patina volume fractions of the studied ancient brass ingots were obtained.

References

[1] E.P. Kazakov, Archaeology of the Eurasian Steppes Journal **1** (2018) 200-210. [*ISSN 2618-9488*]
[2] R. Kotov et al., Proceeding of the 5th International Conference "Archaeometallurgy in Europe", Miskolc, Hungary **73** (2019) 133. [*ISSN 1278-3846*]
[3] V.I. Sidorov, P. P. Starostin, Sovetskaya arheologiya **4** (1970) 233-237. [*ISSN 0038-5034*]
[4] P.M. Valeev, From the history of the early Bulgars (Moscow, 1981) 83 p.
[5] N.V. Eniosova et al., Neskonchaemoe leto: sbornik statei v chest' Eleny Aleksandrovny Rybinoi (Veliky Novgorod, Typography Lyubavich, 2018) 62-73. [*ISBN 978-5-86983-848-3*]
[6] M. Mednikova et al., Journal of Imaging, **6(6)** (2020) 45. [*CrossRef*]
[7] N. Kardjilov, G. Festa, Neutron Methods for Archaeology and Cultural Heritage (Springer, Cham, Switzerland, 2017) 349 p. [*CrossRef*]

[8] E. Lehmann et al., Physics Procedia **88** (2017) 5-12. [*CrossRef*]

[9] B. Bakirov et al., Journal of Imaging **7(8)** (2021) 129. [*CrossRef*]

[10] S. Kichanov et al., Journal of Imaging, **4**(2) (2018) 25. [*CrossRef*]

[11] B.A. Bakirov et al., Journal of Surface Investigation: X-ray, Synchrotron and Neutron Techniques **14** (2020) 376-381. [*CrossRef*]

[12] D. Kozlenko et al., Crystals **8(8)** (2018) 331. [*CrossRef*]

[13] D.P. Kozlenko et al., Crystallography Reports **66** (2021) 303-313. [*CrossRef*]

[14] J. Rodriguez-Carvajal, Physica B: Condensed Matter **192** (1993) 55-69. [*CrossRef*]

[15] D.P. Kozlenko et al., Physics of Particles and Nuclei Letters **13** (2016) 346-351. [*CrossRef*]

[16] D.P. Kozlenko et al., Physics Procedia, **69** (2015) 87-91. [*CrossRef*]

[17] K.M. Podurets et al., Crystallography Reports **66** (2021) 254-266. [*CrossRef*]

[18] C.A. Schneider et al., Nature Methods **9(7)** (2012) 671-675. [*CrossRef*]

[19] F. Brun et al., Advanced Structural and Chemical Imaging **3(1)** (2017) 4. [*CrossRef*]

[20] M.G. Abramson et al., Journal of Surface Investigation: X-ray, Synchrotron and Neutron Techniques **12** (2018) 114-117. [*CrossRef*]

[21] T. Hardi P, M. Wibisono, Proceedings of the International Conference on Materials Science and Technology, Jakarta, Indonesia (2010) 137-142. [*ISBN 978-602-97444-3-9*]

[22] E.R. Caley, Proceedings of the American Philosophical Society, JSTOR **84(5)** (1941) 689-761. [*ISSN 0003-049X*]

[23] T. Chang et al., Corrosion Science, **166** (2020) 108477. [*CrossRef*]

[24] V. Morton, Brass from the Past: Brass made, used and traded from prehistoric times to 1800 (Oxford: Archaeopress, 2019) 370 p. [*ISBN 978-1789691566*]